ISSN 1068-1620, Russian Journal of Bioorganic Chemistry, 2020, Vol. 46, No. 4, pp. 627–641. © Pleiades Publishing, Ltd., 2020.

A Novel 2-Phenyl-1,2,3-Triazole Derived Fluorescent Probe for Recyclable Detection of Al^{3+} in Aqueous Medium and Its Application

Zhengfeng Xie[a, 1], Yunpeng Hao[a], Zhen Li[b], Fanghua Sun[a], Junchi Ma[a], Xin Chen[a], Wei Shi[a], and Shun Feng[b, 2]

[a] *Oil and Gas Field Applied Chemistry Key Laboratory of Sichuan Province, College of Chemistry and Chemical Engineering, Southwest Petroleum University, Chengdu, 610500 China*

[b] *School of Life Science and Engineering, Southwest Jiaotong University, Chengdu, 610031 China*

Received July 25, 2019; revised August 9, 2019; accepted September 16, 2019

Abstrast—A novel 2-phenyl-1,2,3-triazole derived fluorescent probe **HPTC** ((2-hydroxybenzylidene)-2-phenyl-2*H*-1,2,3-triazole-4-carbohydrazide) has been designed and synthesized for recyclable detection of Al^{3+} in DMSO/Tris-HCl (pH 7.4) 1 : 100 v/v with high sensitivity and selectivity. A fluorescence enhancement of 97 folds at 457 nm can be realized upon addition of 10.0 equiv. Al^{3+} with excitation at 375 nm. The binding constant of **HPTC** with Al^{3+} and the detection limit of **HPTC** toward Al^{3+} were 1.67×10^5 M^{-1} and 8.875×10^{-8} M, respectively. In addition, the probe **HPTC** can detect Al^{3+} repeatedly in DMSO/Tris-HCl (pH 7.4) 1 : 100 v/v and the detection effect is not changed. The probe **HPTC** showed an excellent detection ability in a wide pH range from 3 to 10 and also in living cells. Furthermore, the Al^{3+} sensing mechanism was confirmed based on Job's plot, ^{1}H NMR titration, HR-MS, and DFT studies. Finally, **HPTC**-doped agarose hydrogel experiment suggests that the **HPTC** can recognize the Al^{3+} in solid state.

Keywords: fluorescent probe, 2-phenyl-1,2,3-triazole, aluminum ion, bioimaging

DOI: 10.1134/S1068162020040214

INTRODUCTION

As the third most abundant metal in the crust, aluminum is extensively used in industries and modern daily life, such as alloy materials, conductive materials, packaging materials, pharmaceuticals, food additives, water purifying agent, etc. [1–8]. Because of the wide application of aluminum, the research has found that when the concentration of Al^{3+} is present in overload quantities, it can cause serious risks to the health of animals and plants and even put away with many species in the ecosystem [9–11]. The excessive Al^{3+} in the human body may also lead to the emergence of diseases, such as Alzheimer's disease, neurasthenia, breast cancer, osteomalacia, and Parkinson's disease. Hence, it is urgently desirable to synthesize a high sensitivity, good selectivity, simplicity, wide range of pH, and short-time Al^{3+} fluorescent probe in environmental and biological systems [12, 13].

In recent years, a series of probes for Al^{3+} have been reported, including imine [14–19], acylhydrazone [20], carbon dots [21], metal-organic framework [22], and photochromic diarylethene [23] probes. Among them, acylhydrazone compounds have gained interest due to the CONHN=CH moiety with strong coordination power and relative ease of synthesis; until now, julolidine [24], chromen [20, 25, 26], pyrazine [27, 28], pyridine [29], benzothiazole [30], rhodamine [31–34], naphthalene [35–39], naphthalimide [13], and benzene [40–42] have been employed as the fluorophore, and the acylhydrazone structure has been adopted as a selectively reactive moiety.

Recently, we have reported a series of highly selective and sensitive fluorescence probes [43–50], some of them based on 2-phenyl-1,2,3-triazole-4-yl backbone, which is a novel fluorophore with strong emission and good conjugation [51, 52]. In 2016, we designed and synthesized a novel fluorescent probe 2-hydroxy-((2-phenyl-2*H*-1,2,3-triazol-4-yl)methylene)benzohydrazide by the condensation reaction of phenyl-2*H*-1,2,3-triazole-4-carbaldehyde and salicylhydrazide. This acylhydrazone-based probe responded to Al^{3+} in ethanol with excellent selectivity and low detection limit [53]. Here, in continuation of our previous research, we synthesized (2-hydroxyben-

[1] Corresponding author: phone: +86 28 83037306; fax: +86 28 83037305; e-mail: xiezhf@swpu.edu.cn.

[2] Corresponding author: e-mail: fengshunxd@hotmail.com.

zylidene)-2-phenyl-2*H*-1,2,3-triazole-4-carbohydrazide (HPTC) by condensation reaction of 2-phenyl-2*H*-1,2,3-triazole-4-carbohydrazide with salicylaldehyde. The probe possessed the 2-phenyl-1,2,3-triazole unit as a fluorophore and CONHN=CH skeleton as recognition site. In Table 1, we summarize some Al^{3+} probes containing the CONHN=CH skeleton with comparison to the probe synthesized in this paper. From the Table 1 we can find that as long as there is a chromophore with oxygen, nitrogen, or sulfur atoms on either side of the CONHN=CH skeleton, it could usually be used as an aluminium ion probe, and the large conjugated chromophore is beneficial to the bathochromic shift of fluorescence emission. Here, the HPTC probe is shown to exhibit high sensitivity and selectivity in aqueous medium with a wide pH range from 3 to 10 by cyclic detection and also applied in living cells.

EXPERIMENTAL

Materials and Apparatus

All reagents and solvents were supplied by Adamas Chemical Co. and used without purification. All of the metal ions were dissolved in distilled water (10 mL) to afford 1×10^{-1} mol/L aqueous solution from their hydrochloride or nitrate salts.

IR spectra (ν, cm^{-1}) were recorded on an Equinox 55 FT-IR spectrometer with KBr pellets. Absorption spectra were obtained by a Metash UV-6000 pc UV-Vis spectrometer. Fluorescence spectra were obtained by a F-320 spectrometer (Gangdong Technology). The ^{13}C NMR and ^{1}H NMR spectra (δ, ppm) were obtained from a VARIAN Inova-400 spectrometer. Bioimaging was obtained with an Olympus CKX41 fluorescence microscope (Tokyo, Japan). HR-MS (TOF-MS) spectra were recorded on a Waters Q-TOF Premier apparatus.

Synthesis

Synthesis of HPTC

The synthetic route of HPTC ((2-hydroxybenzylidene)-2-phenyl-2*H*-1,2,3-triazole-4-carbohydrazide) is shown in Scheme 1. Glacial acetic acid (0.5 mL) was added to a solution of 2-phenyl-2*H*-1,2,3-triazole-4-carbohydrazide (0.203 g, 1 mmol) and 2-hydroxybenzaldehyde (0.135 g, 1.11 mmol) in 5 mL ethanol, and the reaction was refluxed for 6 h. After cooling to room temperature, the precipitate was filtered and washed with cold ethanol to afford the white solid powder in 83.9% yield. mp 198–200°C. IR: 3242, 1632, 1544, 1491, 1305, 755. ^{1}H NMR (400 MHz, DMSO-d_6): 12.34 (s, 1 H), 11.07 (s, 1 H), 8.77 (s, 1 H), 8.62 (s, 1 H), 8.14 (d, J = 8.0 Hz, 2 H), 7.62–7.66 (m, 2 H), 7.58–7.60 (m, 1 H), 7.50–7.54 (m, 1H), 7.30–7.34 (m, 1 H), 6.91–6.94 (m, 2 H). ^{13}C NMR (100 MHz, DMSO-d_6): 157.60, 155.63, 148.99, 143.00, 139.00, 137.33, 131.85, 130.06, 129.33, 129.01, 119.61, 119.29, 118.97, 116.61. HR-MS (TOF-MS+), m/z: $[M + Na]^+$ calcd. for $C_{16}H_{13}N_5O_2Na$ 330.0967, found 330.0955, $[M + H]^+$ calcd. for $C_{16}H_{14}N_5O_2$ 308.1142, found 308.1132.

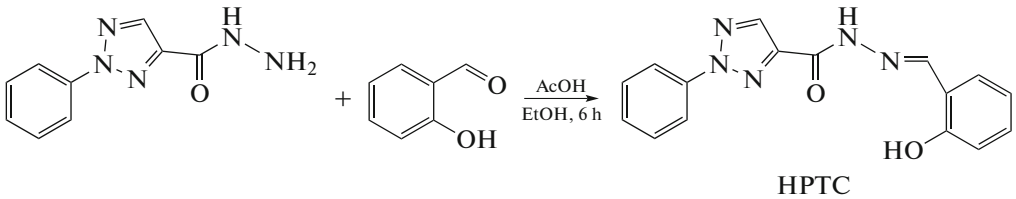

Scheme 1. The synthetic procedure for receptor HPTC.

Intracellular Imaging

HeLa cells were seeded into a 96-well plate and cultured in DMEM medium supplemented with 10% FBS for 24 h. Before in vitro experiments, the cells were incubated for 1 h except that 10 μM HPTC was added in the medium. After incubation, it was rinsed thrice with bioclean PBS buffer, and then further incubated for additional 1 h in the medium containing 30 μM Al^{3+}. After being rinsed again with PBS buffer, inverted fluorescence microscope with a 40× lens (375 nm excitation) was used to obtain fluorescence intracellular images of the cells. The cells were cul-

Table 1. Examples for detection of Al^{3+} by acylhydrazone-based probes

Materials	Solvent, v/v	Type	Detection limit, M	pH	λ_{em}, nm	Reversibility	Response time	Ref.
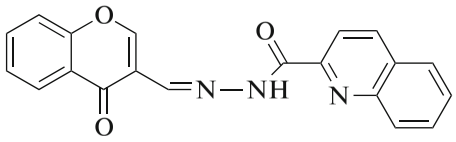	MeOH : H_2O 1 : 20, HEPES buffer pH 7.2	Turn on	7.6×10^{-9}	4–8	520	No		[20]
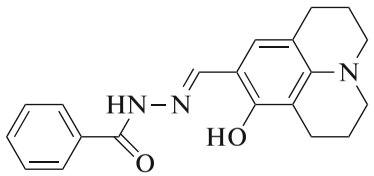	Bis-tris buffer : methanol 999 : 1	Turn on	1.93×10^{-7}	4–10	483	No	–	[24]
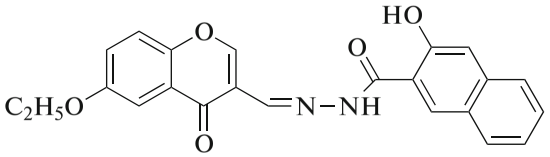	EtOH : H_2O 3 : 1	Turn on	1.82×10^{-7}	5–8	508	No		[25]
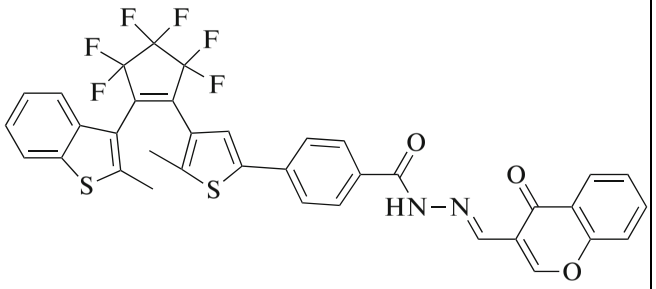	CH_3CN	Turn on	5.47×10^{-7}	–	525	No	–	[26]
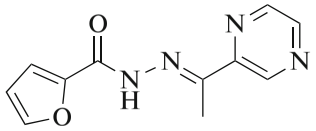	EtOH	Turn on	10^{-7}	–	517	Yes	–	[27]
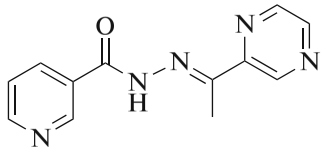	EtOH	Turn on	10^{-7}	–	490	Yes	–	[28]

Table 1. (Contd.)

Materials	Solvent, v/v	Type	Detection limit, M	pH	λ_{em}, nm	Reversibility	Response time	Ref.
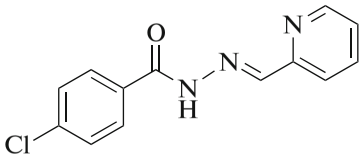	EtOH	Turn on	2×10^{-7}	5–9	435	No	1 min	[29]
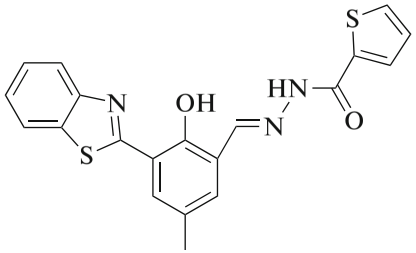	HEPES buffer pH 7.4	Turn on	2.2×10^{-6}	7.4	476	Yes	–	[30]
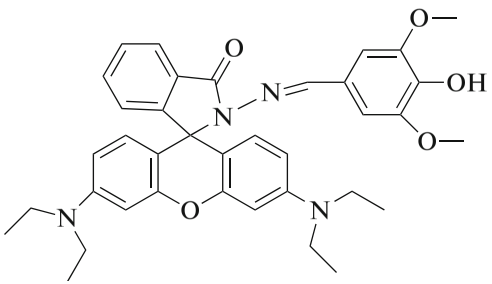	EtOH : HEPES solution 1 : 5	Turn on	1.0568×10^{-8}	7.4	585	Yes	–	[31]
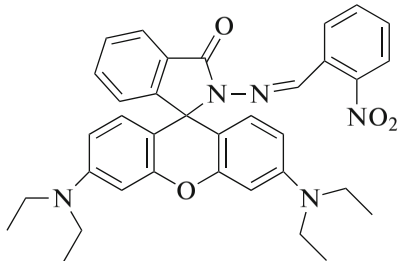	EtOH : H_2O 1 : 3 (HEPES buffer)	Turn on	6.037×10^{-8}	6–10	590	No	–	[32]

Table 1. (Contd.)

Materials	Solvent, v/v	Type	Detection limit, M	pH	λ_{em}, nm	Reversibility	Response time	Ref.
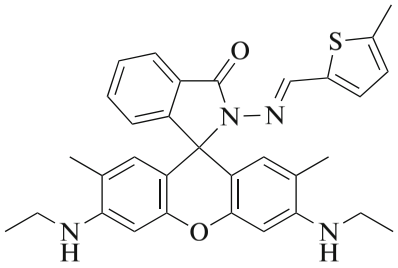	DMF	Turn on	4.17×10^{-6}	–	558	Yes	30 mins	[33]
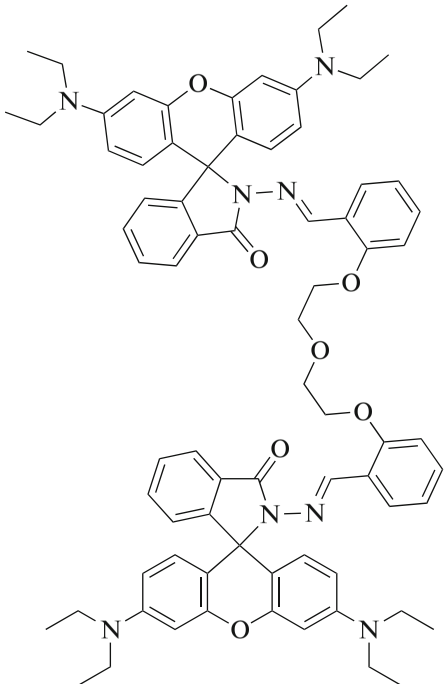	MeOH : DMSO 99 : 1	Turn on	5.0×10^{-7}	2–6	587	Yes	1 min	[34]
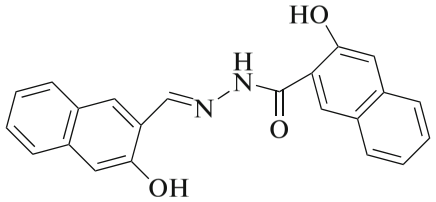	DMSO : H_2O 9 : 1	Turn on	3.66×10^{-6}	–	491	No	1 h	[35]

Table 1. (Contd.)

Materials	Solvent, v/v	Type	Detection limit, M	pH	λ_{em}, nm	Reversibility	Response time	Ref.
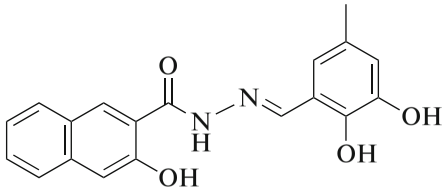	THF : H_2O 6 : 4 (HEPES buffer)	Turn on	0.92×10^{-9}	4–12	486	No	–	[36]
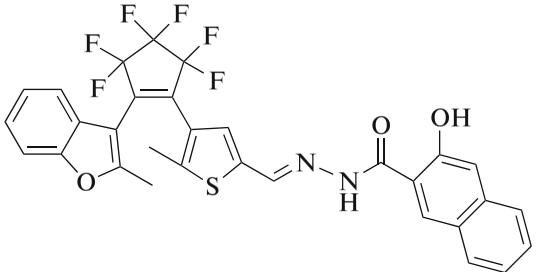	MeOH	Turn on	2.2×10^{-9}	–	563	No	–	[37]
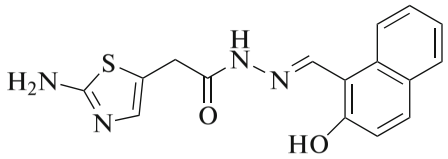	Tris-HCl buffer solution	Turn on	1.09×10^{-9}	7.4	451	No	–	[38]
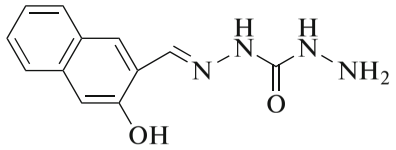	DMSO : HEPES 1 : 99	Turn on	1.89×10^{-8}	5–9	445	Yes	1 min	[39]
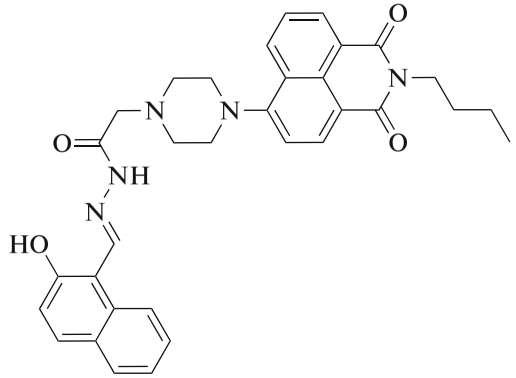	CH_3OH	Turn on	7.4×10^{-9}	–	508	No	10 min	[13]

Table 1. (Contd.)

Materials	Solvent, v/v	Type	Detection limit, M	pH	λ_{em}, nm	Reversibility	Response time	Ref.
β-CD-L 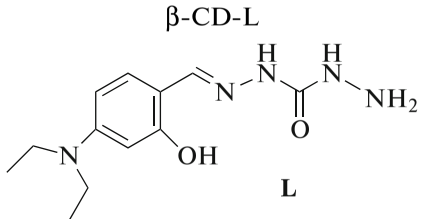 L	HEPES buffer solution	Turn on	10^{-7}	7.2	425	No	–	[40]
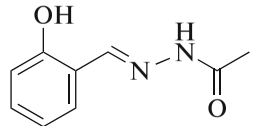	Pure water	Turn on	5×10^{-10}	–	441	No	–	[41]
TEPA-β-CD-L 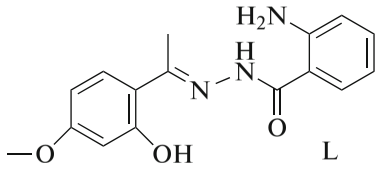 L	Aqueous media	Turn on	1×10^{-7}	7.2	405–425	No	–	[42]
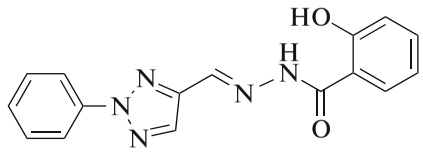	EtOH	Turn on	1.2×10^{-8}	–	442	No	Immediately	[53], our work
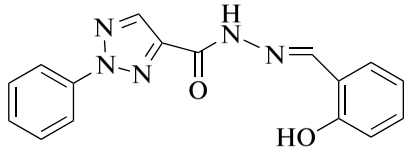	DMSO/H_2O (1 : 100, v/v, Tris-HCl buffer, pH 7.4)	Turn on	8.875×10^{-8}	3–10	457	Yes	Immediately	This work

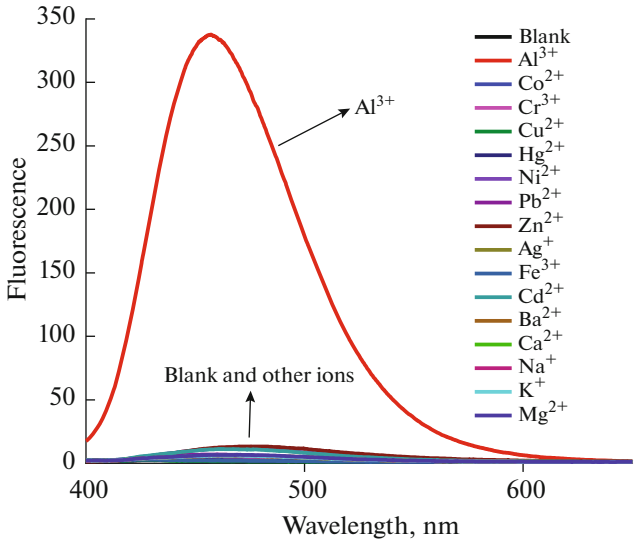

Fig. 1. Fluorescence spectra (λ_{ex} = 375 nm) of HPTC (10.0 μM) and upon the addition of metal ions (10.0 equiv.) of Cr^{3+}, Ag^{+}, Ba^{2+}, Ca^{2+}, Cd^{2+}, Co^{2+}, Cu^{2+}, Fe^{3+}, Hg^{2+}, K^{+}, Na^{+}, Mg^{2+}, Ni^{2+}, Pb^{2+}, Zn^{2+}, and Al^{3+} in DMSO/Tris-HCl buffer (pH 7.4) 1 : 100, v/v.

tured and incubated were all done at 37°C under 5% CO_2 in a humidity incubator.

HPTC Doped Agarose Gels

With the following method, HPTC-doped agarose gels were obtained. Agarose 20 mg was thoroughly dissolved in 2 mL of boiling water. After the aqueous solution was cooled to 70°C, 40 μL of HPTC solution in DMSO (10.0 mM) was added and the mixture was rapidly stirred with ultrasound for 2 min. Then the aqueous solution was placed at room temperature until the gel was formed.

RESULT AND DISCUSSION

Fluorescence Studies

Optical properties of the HPTC probe. HPTC (3.07 mg, 0.01 mmol) was dissolved in DMSO (10 mL) and 20 μL of this solution was diluted with 2 mL Tris-HCl buffer (pH 7.4). Fluorescence spectra of HPTC with various metal ions (Ag^{+}, Al^{3+}, Ba^{2+}, Ca^{2+}, Cd^{2+}, Co^{2+}, Cu^{2+}, Fe^{3+}, Hg^{2+}, K^{+}, Mg^{2+}, Ni^{2+}, Pb^{2+}, Zn^{2+}, Na^{+}, and Cr^{3+}) in 100 : 1 (v/v) Tris-HCl buffer (pH 7.4) : DMSO were recorded and the remarkable enhancement in fluorescence intensity (ca. 97-folds) was discovered only in the presence of Al^{3+} (Fig. 1). This fluorescence enhancement could be explained by the chelation-enhanced fluorescence (CHEF) through the coordination of hydrazide-O, azomethine-N, and phenolic hydroxyl-O to Al^{3+} ion [20, 24]. The solution of HPTC demonstrated a significant fluorescence enhancement from colorless to bright blue in the presence of Al^{3+}, while other ions did not enhance fluorescence, which could easily be discriminated with bare eye under the ultraviolet lamp (Fig. 2). Therefore, the probe exhibited excellent selectivity for Al^{3+} compared with other metal ions.

The competition experiments. Competition experiments were applied to prove the possibility of using HPTC as a valuable selective fluorescent probe for Al^{3+}. For this reason, HPTC was treated with

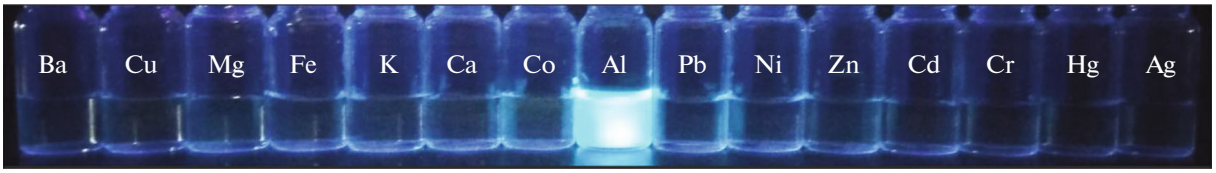

Fig. 2. Photographs of the fluorescence of HPTC (10.0 μM) in the presence of various metal ions (10.0 equiv.) under portable UV lamp.

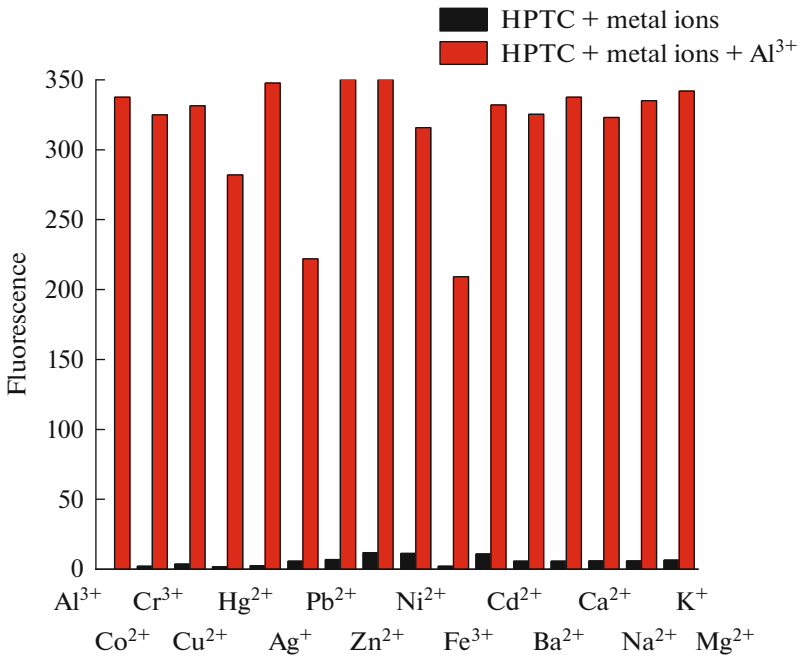

Fig. 3. Interference from other metal cations in a binary mixture in DMSO/Tris-HCl buffer (pH 7.4) 1 : 100, v/v: HPTC (10.0 μM) + Al^{3+} (10.0 equiv.) + M^{n+} (10.0 equiv.), where $M^{n+} = Ag^+$, Ba^{2+}, Ca^{2+}, Cd^{2+}, Co^{2+}, Cu^{2+}, Fe^{3+}, Hg^{2+}, K^+, Mg^{2+}, Ni^{2+}, Pb^{2+}, Zn^{2+}, Na^+, Cr^{3+} (λ_{ex} = 375 nm).

10.0 equiv. Al^{3+} in the presence of 10.0 equiv. other metal ions in DMSO/Tris-HCl buffer (pH 7.4) 1 : 100, v/v, solution. The competitive metal ions were first added to the HPTC solution and then the Al^{3+} ion was put in the solution. As shown in Fig. 3, the HPTC probe could efficiently detect Al^{3+} ion and no interference was observed. This result also demonstrated that the probe exhibited excellent selectivity for Al^{3+}.

Titrations experiments. In fluorescence titration experiments of HPTC with increasing concentrations of Al^{3+} from 0 to 2×10^{-4} M, the fluorescence emission intensity at 457 nm grew gradually (Fig. 4a), demonstrating successful coordination. The binding constant of HPTC with Al^{3+} was calculated as 1.67×10^5 M^{-1} by the Benesi–Hildebrand equation [25], and the detection limit of HPTC toward Al^{3+} was also calculated as 8.875×10^{-8} M according to the equation $DL = 3\sigma/k$ [54].

The effect of pH. To explore whether the different pH environments have effect on the detection of Al^{3+}, the influence of pH on the fluorescence was studied. The fluorescence intensity of HPTC in the absence and presence of $Al^{3+}$was investigated. In Fig. 5, it is clear that HPTC itself has no fluorescence in a wide pH range from 3 to 10; when 10 equiv. of Al^{3+} was added, the fluorescence intensity has greatly increased, which demonstrates that HPTC can be employed to detect Al^{3+} in a wide range of pH 3 to 10 and without any interference. Of course, HPTC could be used under physiological conditions.

Cyclic detection capability. For purpose of finding practical application for HPTC, the cyclic detection of Al^{3+} by HPTC was investigated. As shown in Fig. 6, addition of 10 equiv. EDTA to the solution of HPTC–Al^{3+} resulted in quenching of the fluorescence emission intensity, indicating the regeneration of HPTC. Nevertheless, when 10 equiv. Al^{3+} was added to the regenerated HPTC, the enhancement of the fluorescence luminance occurred again at 457 nm. Alternately adding Al^{3+} (10 equiv.) and EDTA (10 equiv.) for 5 times did not reduce sensitivity of HPTC considerably.

For this reason, it was concluded that HPTC could be employed as a recyclable fluorescent probe with high selectivity and sensitivity for Al^{3+} in a wide pH range over other environmental and biological metal ions.

Job's plot measurement. The binding stoichiometry between the receptor HPTC and the aluminum ion was confirmed by the Job's plot. As depicted in Fig. 7, the fluorescence emission intensity at 457 nm reached maximum when the molecular fraction of HPTC was 0.5, which indicated that HPTC and Al^{3+} formed a 1 : 1 complex.

^{1}H NMR titration experiments. ^{1}H NMR titration experiments were carried out for the sake of elucidation of the mechanism of the HPTC–Al^{3+} complex formation. As shown in Fig. 8, when 1.0 equiv. Al^{3+} was added to HPTC, the –OH proton signal at

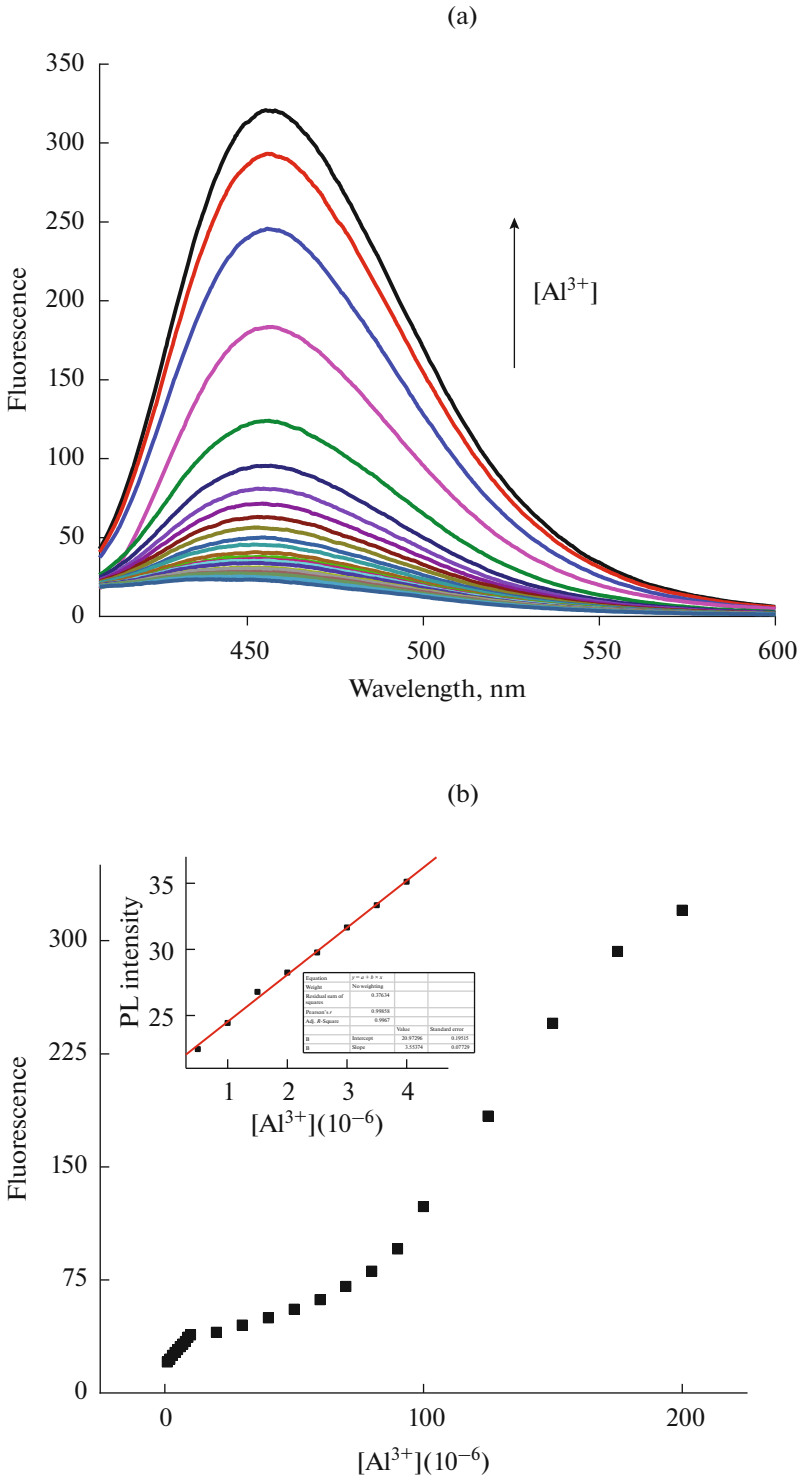

Fig. 4. (a) Fluorescence spectra of **HPTC** (10.0 μM) in DMSO/Tris-HCl buffer (pH 7.4) 1 : 100, v/v, upon the addition of $Al(NO_3)_3$ with an excitation at 375 nm. (b) Fluorescence intensity at 457 nm versus the molar concentration of Al^{3+} added. Insert: enlarged figure in the concentration range of 5×10^{-7}–4×10^{-6} M of Al^{3+}.

11.06 ppm almost disappeared owing to its strong involvement in bonding with Al^{3+} [18, 24, 35], but the –NH proton remained unchanged owing to its non-involvement in bonding with Al^{3+}. The results illustrate that the two oxygen atoms (–OH and C=O) and the nitrogen atom (C=N) are coordinated with Al^{3+}.

To explore the constituent of the HPTC-Al^{3+} formed in the solutions, the HR-MS spectra was recorded, the peak with a 75% intensity at m/z = 428.0968 (calcd. 428.1009) is attributed to the formula $[AlNO_3(HPTC)(CH_3OH)]$. This prove the binding stoichiometry of HPTC–Al^{3+} is 1 : 1 (Scheme 2).

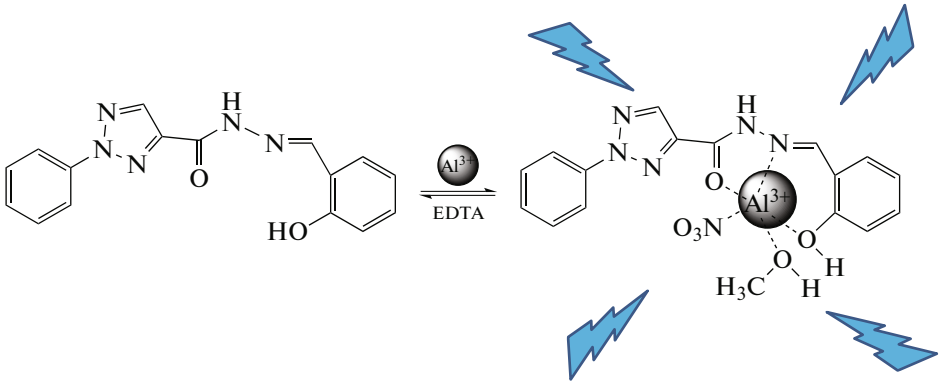

Scheme 2. The proposed mechanism of the HPTC–Al^{3+} complex formation.

Density functional theory (DFT) studies. Optical properties of HPTC and HPTC–Al^{3+} could be explained through a theoretical calculation. The structures of HPTC and HPTC–Al^{3+} were optimized by DFT calculation with the B3LYP method. It was found that the computed HOMO and LUMO band gap energy of the HPTC (0.091 eV) is higher than that of the HPTC–Al^{3+} (0.009 eV). Similar phenomena have been reported [16, 20, 36, 38]. The fluorescence enhancement of HPTC–Al^{3+} may be attributed to intramolecular charge transfer (ICT) in HPTC. The binding of HPTC with Al^{3+} causes the reduction of the oxidation potential and the increase of the electron acceptability. Therefore, electron transfer becomes easier and the fluorescence emission is enhanced (Fig. 9).

HeLa Cells Imaging Studies

Because HPTC was highly selective and sensitive for Al^{3+} ions, we decided to examine the turn-on sensing of Al^{3+} ions in HeLa cells. As Fig. 10b shows, when HeLa cells were incubated with HPTC (10 μM) for 1 h at 37°C, no fluorescence was observed. Then, the binding interactions of HPTC (10 μM) with Al^{3+} ions (30 μM) in living cells were investigated; strong blue fluorescence was observed in the HeLa cells

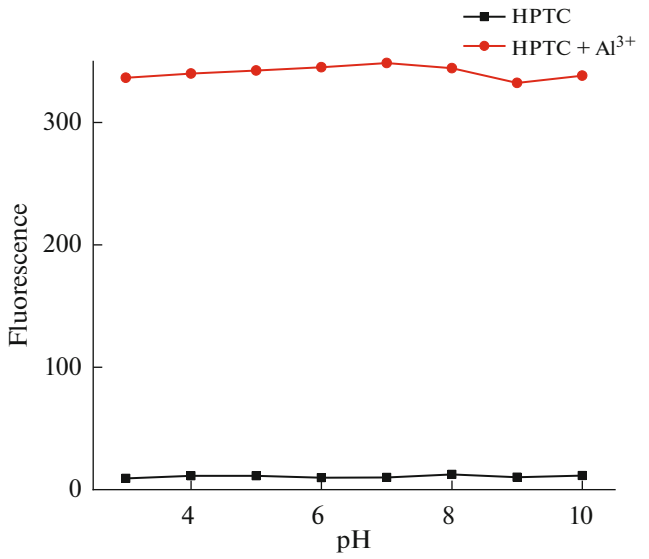

Fig. 5. Effect of pH on fluorescence intensity of the HPTC–Al^{3+} complex in DMSO/Tris-HCl buffer (pH 7.4) 1 : 100, v/v.

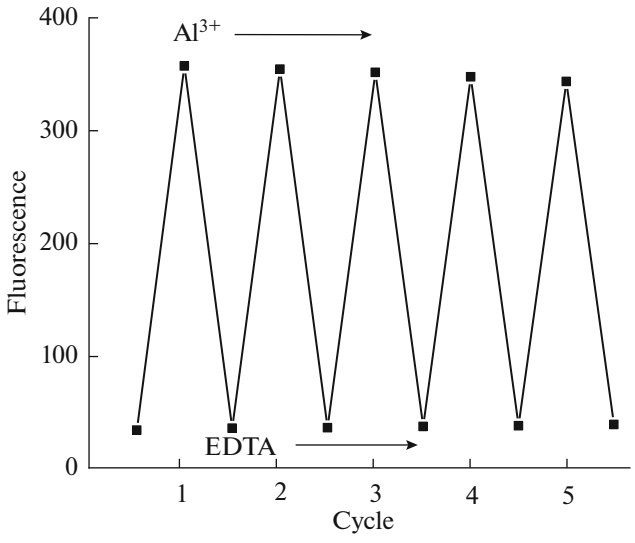

Fig. 6. Fluorescence intensity changes of HPTC ($1.0 \times 10^{-}$M) upon alternate addition of $Al^{3+}$and EDTA (10 equiv.) in DMSO/Tris-HCl buffer (pH 7.4) 1 : 100, v/v.

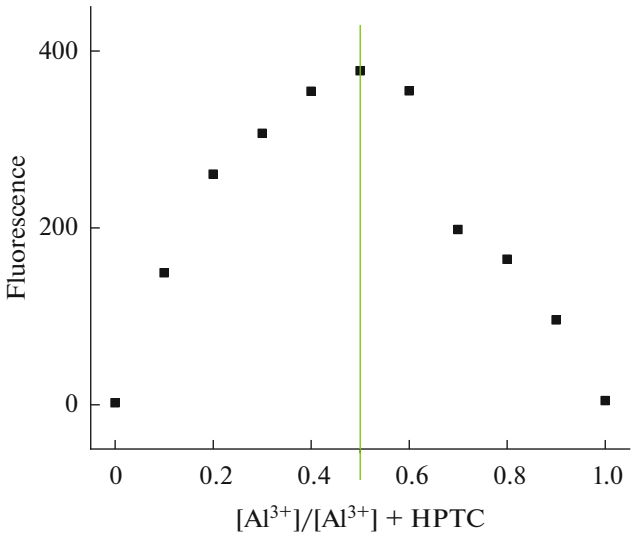

Fig. 7. Job's plot for the determination of the stoichiometry of HPTC and Al^{3+} in the complex.

(Fig. 10e). The results demonstrate that HPTC can be used to detect Al^{3+} in living HeLa cells.

Al^{3+} Detection by HPTC-Doped Agarose Hydrogels

Inspired by the successful application of HPTC to detect Al^{3+} in aqueous medium, we further tested Al^{3+} in solid state. The HPTC-doped agarose hydrogels (HPTC with an average concentration of 0.2 mM per gel) were prepared to detect Al^{3+}. These gels were immersed in Al^{3+} aqueous solutions of various concentrations with pH 7.4. Under the irradiation of UV lamp (365 nm excitation), the fluorescence becomes more and more bright with the increase of the concentration of Al^{3+} (Fig. 11). Therefore, the HPTC probe could be applied to detect Al^{3+} in actual samples.

CONCLUSION

A novel probe HPTC based on acylhydrazone structure was designed and synthesized by a facile condensation reaction. HPTC exhibited excellent selectivity and sensitivity for Al^{3+} without interference with 97-folds fluorescence enhancement in aqueous medium, and was efficient under recycling conditions, in a wide range of pH, and in cellular environment.

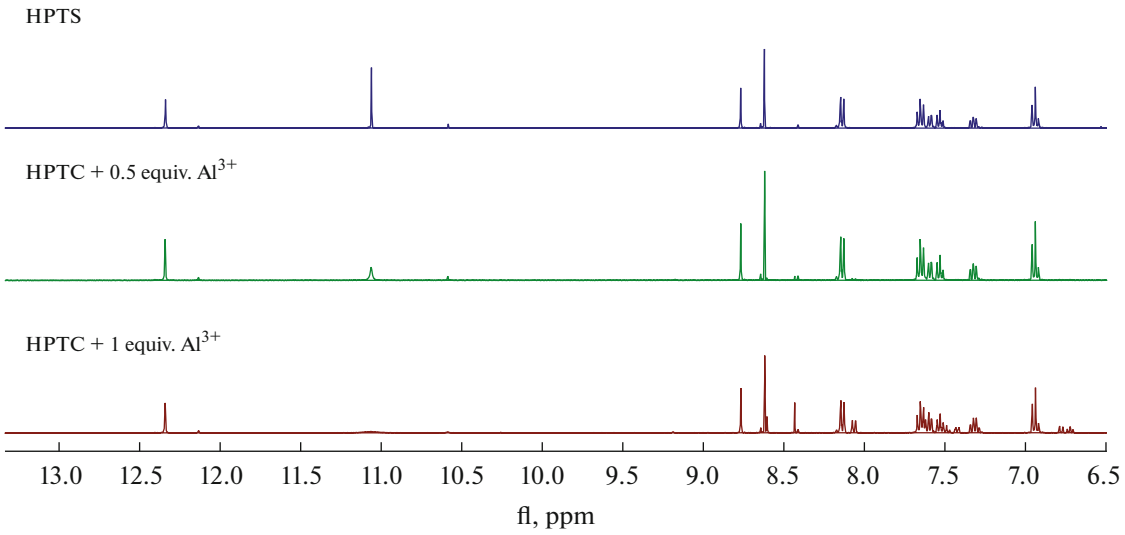

Fig. 8. ^1H NMR spectral patterns upon adding 0 to 1 equiv. of Al^{3+} in DMSO-d_6.

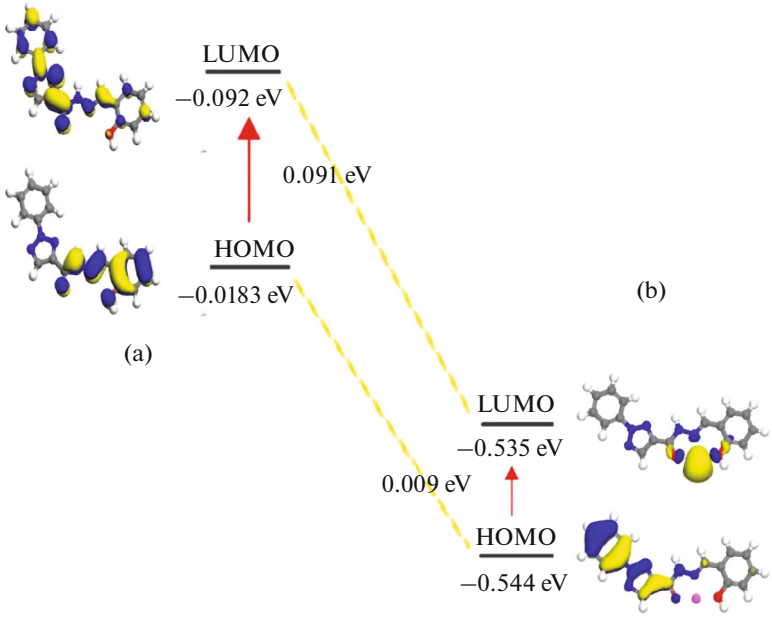

Fig. 9. The display of HOMO and LUMO of HPTC (a) and HPTC–Al^{3+} (b).

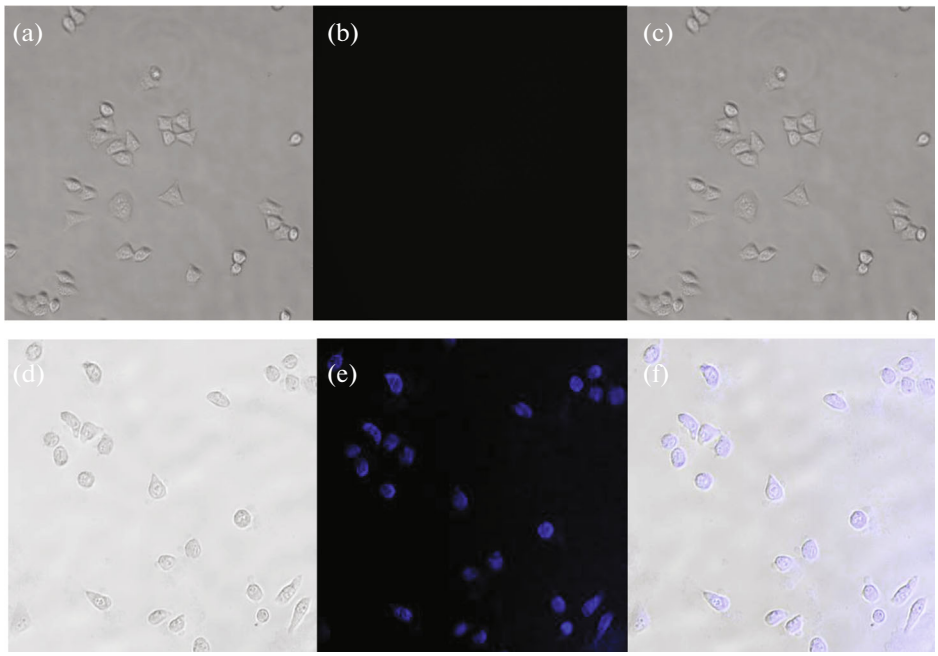

Fig. 10. Fluorescence and bright-field images of HeLa cells stained with HPTC (a–c) and with both HPTC and Al^{3+} (d–f). Left, bright field image; center, fluorescence image; right, merged image. [HPTC] = 10 μM, [Al^{3+}] = 30 μM. Excitation wavelength 375 nm.

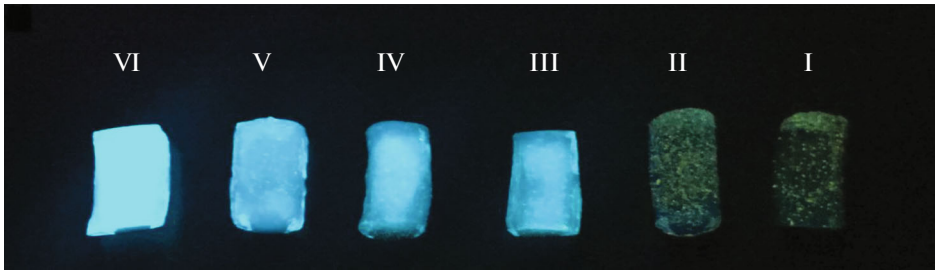

Fig. 11. Visual detection of Al^{3+} using HPTC-doped agarose hydrogels under 457 nm UV light (from I to VI: 0, 0.00002, 0.0002, 0.002, 0.02, 0.2 mM).

The results of HPTC-doped agarose hydrogels for Al^{3+} indicate that HPTC has good application value.

FUNDING

The authors thank Youth Science and Technology Innovation Team of SWPU (project no. 2017CXTD05).

COMPLIANCE WITH ETHICAL STANDARDS

This article does not contain any studies involving animals or human participants performed by any of the authors.

Conflict of Interests

The authors declare that they have no conflict of interests.

REFERENCES

1. Rao, V.K., Rao, A.J., Reddy, S.S., Raju, C.N., Rao, P.V., and Ghosh, S.K., *Eur. J. Med. Chem.*, 2010, vol. 45, pp. 203–209. https://doi.org/10.1016/j.ejmech.2009.09.045
2. Lee,Y.J., Lim, C., Suh, H., Song, E.J., and Kim, C., *Sens. Actuators. B Chem.*, 2014, vol. 201, pp. 535–544. https://doi.org/10.1016/j.snb.2014.05.035
3. Li, C.R., Qin, J.C., Wang, G.Q., Wang, B.D., Fu, A.K., and Yang, Z.Y., *Inorg. Chim., Acta*. 2015, vol. 430, pp. 91–95. https://doi.org/10.1016/j.ica.2015.02.004
4. Liu, C., Yang, Z., and Yan, M., *J. Coord. Chem.*, 2012, vol. 65, pp. 3845–3850. https://doi.org/10.1080/00958972.2012.726987
5. Lu, C.Y., Liu, Y.W., Hung, P.J., Wan, C.F., and Wu, A.T., *Inorg. Chem. Commun.*, 2013, vol. 35, pp. 273–275. https://doi.org/10.1016/j.inoche.2013.06.005
6. Maity, D. and Govindaraju, T., *Inorg. Chem.*, 2010, vol. 49, pp. 7229–7231. https://doi.org/10.1021/ic1009994
7. Malkondu, S., *Tetrahedron*, 2014, vol. 70, pp. 5580–5584. https://doi.org/10.1016/j.tet.2014.06.094
8. Qin, J.C., Li, T.R., Wang, B.D., Yang, Z.Y., and Fan, L., *Synth. Met.*, 2014, vol.195, pp. 141–146. https://doi.org/10.1016/j.synthmet.2014.06.002
9. Chen, Y., Shi, W., Hui, Y., Sun, X., Xu, L., Feng, L., and Xie, Z., *Talanta*, 2015, vol. 137, pp. 38–42. https://doi.org/10.1016/j.talanta.2015.01.018
10. Ding, W.H., Wang, D., Zheng, X.J., Ding, W.J., Zheng, J.Q., Mu, W.H., Cao, W., and Jin, L.P., *Sens. Actuators. B Chem.*, 2015, vol. 209, pp. 359–367. https://doi.org/10.1016/j.snb.2014.11.144
11. Hu, S., Song, Wu, J.G., Cheng, C., and Gao, Q., *Spectrochim. Acta. A Mol. Biomol. Spectrosc.*, 2015, vol. 136, pp. 1188–1194. https://doi.org/10.1016/j.saa.2014.10.005
12. Lu, Y., Huang, S., Liu, Y., He, S., Zhao, L., and Zeng, X., *Org. Lett.*, 2011, vol. 13, pp. 5274–5277. https://doi.org/10.1021/ol202054v
13. Kang, L., Liu, Y.T., Li, N.N., Dang, Q.X., Xing, Z.Y., Li, J.L., and Zhang, Y., *J. Lumin.*, 2017, vol. 186, pp. 48–52. https://doi.org/10.1016/j.jlumin.2016.12.056
14. Kaur, B., Kaur, N., and Kumar, S., *Coord. Chem. Rev.*, 2018, vol. 358, pp. 13–69. https://doi.org/10.1016/j.ccr.2017.12.002
15. Lee, J.J., Park, G.J., Kim, Y.S., Lee, S.Y., Lee, H.J., Noh, I., and Kim, C., *Biosens. Bioelectron.*, 2015, vol. 69, pp. 226–229. https://doi.org/10.1016/j.bios.2015.02.038
16. Kumar, M., Kumar, A., Faizi, Md.S.H., Kumar, S., Singh, M.K., Sahu, S.K., Kishor, S., and John, R.P., *Sens. Actuators. B Chem.*, 2018, vol. 260, pp. 888–899. https://doi.org/10.1016/j.snb.2018.01.098
17. Selvan, G.T., Kumaresan, M., Sivaraj, R., Enoch, I.V.M.V., and Selvakumar, P.M., *Sens. Actuators. B Chem.*, 2016, vol. 229, pp. 181–189. https://doi.org/10.1016/j.snb.2016.01.097
18. Jo, T.G., Bok, K.H., Han, J., Lim, M.H., and Kim, C., *Dyes pigm.*, 2017, vol. 139, pp. 136–147. https://doi.org/10.1016/j.dyepig.2016.11.052
19. Sarma, S., Bhowmik, A., Sarma, M.J., Banu, S., Phukan, P., and Das, D.K., *Inorg. Chim. Acta*, 2018, vol. 469, pp. 202–208. https://doi.org/10.1016/j.ica.2017.09.025
20. Purkait, R., Patra, C., Mahapatra, A.D., Chattopadhyay, D., and Sinha, C., *Sens. Actuators. B Chem.*, 2018, vol. 257, pp. 545–552. https://doi.org/10.1016/j.snb.2017.10.168
21. Sooksin, S., Promarak, V., Ittisanronnachai, S., and Ngeontae, W., *Sens. Actuators. B Chem.*, 2018, vol. 262, pp. 720–732. https://doi.org/10.1016/j.snb.2018.01.239
22. Lv, R., Chen, Z., Fu, X., Yang, B., Li, H., Su, J., Gu, W., and Liu, X., *J. Solid State Chem.*, 2018, vol. 259, pp. 67–72. https://doi.org/10.1016/j.jssc.2017.12.033
23. Wang, N., Wang, R., Tu, Y., Pu, S., and Liu, G., *Spectrochim. Acta A*, 2018, vol. 196, pp. 303–310. https://doi.org/10.1016/j.saa.2018.02.018
24. Lee, S.A., You, G.R., Choi, Y.W., Jo, H.Y., Kim, A.R., Noh, I., Kim, S.J., Kim, Y., and Kim, C., *Dalton Trans.*, 2014, vol. 43, pp. 6650–6659. https://doi.org/10.1039/C4DT00361F
25. Liu, L.M. and Yang, Z.Y., *Inorg. Chim. Acta*, 2018, vol. 469, pp. 588–592. https://doi.org/10.1016/j.ica.2017.09.051
26. Feng, E., Fan, C., Wang, N., Liu, G., and Pu, S., *Dyes Pigm.*, 2018, vol. 151, pp. 22–27. https://doi.org/10.1016/j.dyepig.2017.12.041
27. Li, C.R., Qin, J.C., Wang, G.Q., Wang, B.D., and Yang, Z.Y., *Anal. Methods*, 2015, vol. 7, pp. 3500–3505. https://doi.org/10.1039/C5AY00200A
28. Li, C.R., Liao, Z.C., Qin, J.C., Wang, B.D., and Yang, Z.Y., *J. Lumin.*, 2015, vol. 168, pp. 330–333. https://doi.org/10.1016/j.jlumin.2015.07.055

29. Liu, Y.J., Tian, F.F., Fan, X.Y., Jiang, F.L., and Liu, Y., *Sens. Actuators. B Chem.*, 2017, vol. 240, pp. 916–925. https://doi.org/10.1016/j.snb.2016.09.051

30. Chen, Y., Wei, T., Zhang, Z., Chen, T., Li, J., Qiang, J., Lv, J., Wang, F., and Chen, X., *Ind. Eng. Chem. Res.*, 2017, vol. 56, pp. 12267–12275. https://doi.org/10.1021/acs.iecr.7b02979

31. Liu, T., Wan, X., and Yao, Y., *Sens. Actuators. B Chem.*, 2018, vol. 254, pp.1094–1100. https://doi.org/10.1016/j.snb.2017.07.114

32. Sen, B., Mukherjee, M., Banerjee, S., Pal, S., and Chattopadhyay, P., *Dalton Trans.*, 2015, vol. 44, pp. 8708–8717. https://doi.org/10.1039/C5DT00315F

33. Li, M.X., Zhang, X., Fan, Y.H., and Bi, C.F., *Luminescence*, 2016, vol. 31, pp. 851–855. https://doi.org/10.1002/bio.3041

34. Mergu, N., Singh, A.K., and Gupta, V.K., *Sensors*, 2015, vol. 15, pp. 9097–9111. https://doi.org/10.3390/s150409097

35. Liao, Z., Liu, Y., Han, S.F., Wang, D., Zheng, J.Q., Zheng, X.J., and Jin, L.P., *Sens. Actuators. B Chem.*, 2017, vol. 244, pp. 914–921. https://doi.org/10.1016/j.snb.2017.01.074

36. Alam, R., Mistri, T., Bhowmick, R., Katarkar, A., Chaudhuri, K., and Ali, M., *RSC Adv.*, 2016, vol. 6, pp. 1268–1278. https://doi.org/10.1039/C5RA18424J

37. Cui, S., Tang, Y., and Pu, S., *RSC Adv.*, 2016, vol. 6, pp. 84592–84598. https://doi.org/10.1039/C6RA18068J

38. Gupta, S.R., Singh, P., Koch, B., and Singh, V.P., *J. Photoch. Photobio. A*, 2017, vol. 348, pp. 246–254. https://doi.org/10.1016/j.jphotochem.2017.08.055

39. Zhu, Z.X., Yu, D.D., Liu, Z.G., Huang, Y.W., Zhou, A.Y., Chen, Z.W., Sun, J., Wang, X., Jin, L.T., and Cong, W.T., *Luminescence*, 2017, vol. 32, pp. 1307–1312. https://doi.org/10.1002/bio.3326

40. Liu, Z.C., Zhu, W.P., Chen, Y.H., Li, Y.X., Ding, Y.J., Yang, W.J., and Li, K., *Dalton Trans.*, 2015, vol. 44, pp. 16528–16533. https://doi.org/10.1039/C5DT02220G

41. Wang, J. and Peng, Y., *RSC Adv.*, 2014, vol. 4, pp. 5845–5848. https://doi.org/10.1039/C3RA47104G

42. Liu, Z., Ren, K., Chen, Y., Li, Y., Xie, J., Ding, Y., Li, L., Li, K., Zhu, W., Yang, W., and Xu, Z., *RSC Adv.*, 2017, vol. 7, pp. 38160–38165. https://doi.org/10.1039/C7RA06915D

43. Yue, Y., Xie, Z., Chu, Y., and Shi, W., *Russ. J. Org. Chem.*, 2019, vol. 55, pp. 866–873. https://doi.org/10.1134/S1070428019060186

44. Chu, Y., Xie, Z., Yue, Y., Yue, Y., Kong, X., Shi, W., and Feng, S., *ACS Omega*, 2019, vol. 4, pp. 5367–5373. https://doi.org/10.1021/acsomega.9b00290

45. Xie, Z., Kong, X., Feng, L., Ma, J., Li, Y., Wang, X., Bao, W., Shi, W., and Hui, Y., *Sens. Actuators. B Chem.*, 2018, vol. 257, pp. 154–165. https://doi.org/10.1016/j.snb.2017.10.167

46. Hao, Y., Xie, Z., Bao, W., Wang, X., and Shi, W., *Chin. J. Org. Chem.*, 2018, vol. 38, pp. 2109–2115. http://sioc-journal.cn/10.6023/cjoc201804034

47. Wang, X., Shi, W., Feng, L., Ma, J., Li, Y., Kong, X., Chen, Y., Hui, Y., and Xie, Z., *Inorg. Chem. Commun.*, 2017, vol. 79, pp. 50–54. https://doi.org/10.1016/j.inoche.2017.03.006

48. Li, Y., Shi, W., Ma, J., Wang, X., Kong, X., Zhang, Y., Feng, L., Hui, Y., and Xie, Z., *J. Photochem. Photobiol. A*, 2017, vol. 338, pp. 1–7. https://doi.org/10.1016/j.jphotochem.2017.01.026

49. Lei, F., Shi, W., Ma, J., Chen, Y., Fan, K., Hui, Y., and Xie, Z., *Sens. Actuators. B Chem.*, 2016, vol. 237, pp. 563–569. https://doi.org/10.1016/j.snb.2016.06.129

50. Lin, H., Shi, W., Tian, Y., Ma, F., Xu, L., Ma, J., Hui, Y., and Xie, Z., *J. Lumin.*, 2015, vol. 157, pp. 280–284. https://doi.org/10.1016/j.jlumin.2014.09.004

51. Yan, W., Wang, Q., Lin, Q., Li, M., Petersen, J.L., and Shi, X., *Chem. Eur. J.*, 2011, vol. 17, pp. 5011–5018. https://doi.org/10.1002/chem.201002937

52. Zhang, Y., Ye, X., Petersen, J.L., Li, M., and Shi, X., *J. Org. Chem.*, 2015, vol. 80, pp. 3664–3669. https://doi.org/10.1021/acs.joc.5b00006

53. Ma, J., Shi, W., Feng, L., Chen, Y., Fan, K., Hao, Y., Hui, Y., and Xie, Z., *RSC Adv.*, 2016, vol. 6, pp. 28034–28037. https://doi.org/10.1039/C6RA01589A

54. Safaeian, M., Solomon, D., and Castle, P.E., *Spectroscopy*, 2003, vol. 18, pp. 112–114. https://www.researchgate.net/publication/279903095_Limits_of_detection_in_spectroscopy.